



IMPROVED DROUGHT EARLY WARNING AND FORECASTING TO STRENGTHEN
PREPAREDNESS AND ADAPTATION TO DROUGHTS IN AFRICA
DEWFORA

A 7th Framework Programme Collaborative Research Project

**Meteorological climate scenarios for Africa and specific case study
regions of the Nile and Niger River basins**

WP3-Task3.2-D3.4

May 2013



Coordinator: Deltares, The Netherlands
Project website: www.dewfora.net
FP7 Call ENV-2010-1.3.3.1
Contract no. 265454





Page intentionally left blank



DOCUMENT INFORMATION

Title	Meteorological climate scenarios for Africa and specific case study regions of the Nile and Niger River basins
Lead Author	Francois Engelbrecht
Contributors	Mogesh Naidoo Mary-Jane Bopape
Distribution	PP
Reference	WP3-Task3.2-D3.4

DOCUMENT HISTORY

Date	Revision	Prepared by	Organisation	Approved by	Notes
18/05/2012		Francois Engelbrecht	CSIR		

ACKNOWLEDGEMENT

The research leading to these results has received funding from the European Union's Seventh Framework Programme (FP7/2007-2013) under grant agreement N°265454



Page intentionally left blank



SUMMARY

Six different CGCM projections of future climate change over Africa have been downscaled to high resolution (50 km in the horizontal) over the African continent, for the period 1961-2100. All six CGCM projections were for the A2 scenario contributed to AR4 of the IPCC. These simulations were subsequently bias-corrected, using the monthly climatologies of rainfall, average temperature and relative humidity of the CRU TS3.1 data set. The projections indicate that drastic climate change, particularly temperature increases, are plausible to occur over Africa during the 21st century, should emissions increase according to or faster, as described in the A2 scenario. The median temperature increase for 2071 to 2100, compared to 1961-1990, varies between 3 and 5 °C across the continent in the CCAM projections. The subtropical regions of the continent (southern Africa and the northern Sahara) are projected to warm most, at a rate of about twice the global rate of temperature increase. That is, drastic increases in surface temperature are likely over the subtropical parts of the continent, even if the UNFCCC would be successful in restraining the global increase in temperature to 2° C. Although the projections of future rainfall changes over the continent show considerable variation across the continent, there are robust signals of some large-scale changes in the CCAM projections. The subtropical parts of the continent (southern Africa and the northern Sahara) are projected to become drier, with even more drastic decreases in rainfall projected for the extra-tropical margins of the continent – the Mediterranean coast of North Africa, and the southwestern Cape and Cape south coast of South Africa. These changes seem to be driven by the strengthening of the subtropical highs in each of the hemispheres, with an associated poleward displacement of the westerly wind regime. There is also a robust signal of East Africa becoming wetter in response to the strengthening of the East African monsoon. More uncertainty surrounds the CCAM projections of future climate change over West Africa and the Sahel, where many CGCMs fail to simulate realistically key aspects of African climate – such as the West African monsoon (e.g. Christensen et al., 2007).

The CCAM projections provide evidence that the frequency of occurrence of very hot days is likely to increase across the continent, and in particular over subtropical southern Africa, the western tropics and North Africa. This is to occur in association with the strengthening of the subtropical highs and the poleward displacement of the westerly wind regime, with associated decreases in rainfall over large parts of the continent. It is likely that extreme rainfall events will increase in frequency across the tropics, in response to the general increase in moisture in the warmer atmosphere. Over East Africa, where the monsoon is projected to strengthen, robust increases in precipitation are projected. Similarly, rainfall increases are projected over the northern parts of Mozambique, due to a northward displacement of tropical cyclone tracks.

The Niger river basin is projected to experience rapid temperature rise during the 21st century, under the A2 scenario. The median of the CCAM ensemble projects temperature increases ranging ranging from 3 °C in the south to 5 °C in the north, under the A2 scenario – a robust message of change across the ensemble members. An associated increase in very hot days (80 days per year or more) is projected for the basin. Such drastic increases in both the average temperature and extreme temperature days are likely to impact negatively on crop yield and the hydrological cycle in the basin (through enhanced evaporation). It is plausible, however, for the basin to experience increases in both annual average rainfall and extreme rainfall events, under enhanced anthropogenic forcing.

The CCAM ensemble projects a robust message of annual rainfall increases, and increases in extreme precipitation events, over the Blue Nile river basin. These increases are projected to occur in response to a strengthening of the East African monsoon. Compared to the Niger basin, less drastic increases in temperature and very hot days are projected for the Blue Nile basin, to some extent as a result of the simulated increases in cloud cover and rainfall over this region.



TABLE OF CONTENTS

summary	5
List of figures	7
1. INTRODUCTION.....	10
2. THE REGIONAL CLIMATE MODEL AND DESIGN OF THE DOWNSCALING EXPERIMENTS	11
2.1 THE CONFORMAL-CUBIC ATMOSPHERIC MODEL.....	11
2.2 BIAS-CORRECTION PROCEDURE.....	13
3. PROJECTIONS OF FUTURE CLIMATE CHANGE OVER AFRICA AND THE DEWFORA CASE STUDY RIVER BASINS	13
3.1 PROJECTED CHANGES IN AVERAGE TEMPERATURE.....	13
3.2 PROJECTED CHANGES IN RAINFALL	14
3.2.1 The Blue Nile river basin and East Africa	15
3.2.2 The Niger river basin, West Africa and the Sahel	15
3.2.3 Southern Africa.....	16
3.2.4 Tropical Africa.....	16
3.2.5 Sahara	16
3.2.6 The African Mediterranean coast	16
4. PROJECTED CHANGES IN EXTREME EVENTS.....	22
5. CONCLUSIONS	27
6. REFERENCES	28

LIST OF FIGURES

Figure 1. Projected change in the annual average maximum temperature over Africa ($^{\circ}\text{C}$), for the periods 2011-2040, 2041-2070 and 2071-2100, relative to 1961-1990. The 90th percentile (upper panel), median (middle panel) and 10th percentile (lower panel) are shown for an ensemble of six downscalings of CGCM projections, for each of the time-slabs. The downscalings were generated using the regional model CCAM. All the CGCM projections contributed to AR4 of the IPCC and are for the A2 SRES scenario.

Figure 2. Projected change in the seasonal average maximum temperatures over Africa ($^{\circ}\text{C}$), for the period 2071-2100, relative to 1961-1990. The 90th percentile (upper panels), median (middle panels) and 10th percentile (lower panels) are shown for an ensemble of six downscalings of CGCM projections, for each of the seasons. The downscalings were generated using the regional model CCAM. All the CGCM projections contributed to AR4 of the IPCC and are for the A2 SRES scenario.

Figure 3. Projected change in the total annual rainfall (mm) over Africa, for the periods 2011-2040, 2041-2070 and 2071-2100, relative to 1961-1990. The 90th percentile (upper panel), median (middle panel) and 10th percentile (lower panel) are shown for an ensemble of six downscalings of CGCM projections, for each of the time-slabs. The downscalings were generated using the regional model CCAM. All the CGCM projections contributed to AR4 of the IPCC and are for the A2 SRES scenario.

Figure 4. Projected change in seasonal rainfall totals (mm) over Africa, for the period 2071-2100 relative to 1961-1990. The 90th percentile (upper panels), median (middle panels) and 10th percentile (lower panels) are shown for an ensemble of six downscalings of CGCM projections, for each of the seasons. The downscalings were generated using the regional model CCAM. All the CGCM projections contributed to AR4 of the IPCC and are for the A2 SRES scenario.

Figure 5. Projected change in the annual frequency of occurrence of extreme rainfall events over Africa, for the periods 2011-2040, 2041-2070 and 2071-2100, relative to 1961-1990. The 90th percentile (upper panel), median (middle panel) and 10th percentile (lower panel) are shown for an ensemble of six downscalings of CGCM projections, for each of the time-slabs. The downscalings were generated using the regional model CCAM. All the CGCM projections contributed to AR4 of the IPCC and are for the A2 SRES scenario. Units are the number of events per grid point per year.

Figure 6. Projected change in the seasonal frequency of occurrence of extreme rainfall events over Africa, for the period 2071-2100 relative to 1961-1990. The 90th percentile (upper panel), median (middle panel) and 10th percentile (lower panel) are shown for an ensemble of six downscalings of CGCM projections, for each of the seasons. The downscalings were generated using the regional model CCAM. All the CGCM projections contributed to AR4 of the IPCC and are for the A2 SRES scenario. Units are the number of events per grid point per year.

Figure 7. Projected change in the annual frequency of occurrence of very hot days over Africa, for the periods 2011-2040, 2041-2070 and 2071-2100, relative to 1961-1990. The 90th percentile (upper panel), median (middle panel) and 10th percentile (lower panel) are shown for an ensemble of six downscalings of CGCM projections, for each of the time-slabs. The downscalings were generated using the regional model CCAM. All the CGCM projections contributed to AR4 of the IPCC and are for the A2 SRES scenario. Units are the number of events per grid point per year.

Figure 8. Projected change in the seasonal frequency of occurrence of very hot days over Africa, for the period 2071-2100, relative to 1961-1990. The 90th percentile (upper panel), median (middle panel) and 10th percentile (lower panel) are shown for an ensemble of six



downscalings of CGCM projections, for each of the seasons. The downscalings were generated using the regional model CCAM. All the CGCM projections contributed to AR4 of the IPCC and are for the A2 SRES scenario. Units are the number of events per grid point per year.





1. INTRODUCTION

The African continent is thought to be highly vulnerable to anthropogenically induced climate change (e.g. Meadows, 2006). The rate of warming over the continent is robustly estimated to be in the order of 1.5 times the global mean rate of temperature increase (Christensen et al., 2007), according to the coupled global climate model (CGCM) projections described in Assessment Report Four (AR4) of the Intergovernmental Panel on Climate Change (IPCC). It seems plausible for large parts of subtropical Africa, including southern Africa and the northern Sahara, to become drier within this generally warmer climate, whilst East Africa is robustly projected to become wetter (e.g. Christensen et al., 2007; Engelbrecht et al., 2009). These changes in African climate may be expected to have wide-ranging implications, including largely negative impacts on agriculture (e.g. Thornton et al., 2011), water security and the abundance and distribution of pests and diseases (e.g. Olwoch et al., 2008).

The CGCM projections described in AR4 and elsewhere are of course horizontal resolution, and therefore to some extent inadequate to describe the regional details of climate change over Africa. Only a few detailed projections of climate change have been obtained to date for parts of the continent, using dynamic regional climate models (e.g. Tadross et al., 2005; Engelbrecht et al., 2009; Engelbrecht et al., 2012). These experiments have mostly focused on the southern African region, and have suggested that it is plausible for the eastern parts of southern Africa to become wetter during summer, with an associated increase in the frequency of occurrence of convective rainfall events (Tadross et al., 2005; Hewitson and Crane, 2006; Engelbrecht et al., 2009). Annual rainfall totals have, consistent with the CGCM projections, been projected to decrease over most of the southern African subcontinent in response to a general strengthening of the subtropical high-pressure belt (e.g. Seidel, 2008; Engelbrecht et al., 2009). This drying is projected to occur despite the projected increase in summer rainfall totals over the eastern parts of the subcontinent.

There is a need for larger ensembles of high-resolution regional projections of climate change to be obtained for the larger African continent, in order to describe more comprehensively the uncertainty range associated with these projections. Now that super-computing facilities are becoming more generally available on the African continent (for example in South Africa, through the computer clusters of the Centre for High Performance Computing (CHPC) of the Meraka Institute of the Council for Scientific and Industrial Research (CSIR)), there is the potential to perform more of these computationally expensive regional climate modelling experiments. FP7 project DEWFORA has the aim of generating very high-resolution projections of regional climate change over key river basins of the continent – in particular the Niger and Blue Nile river basins. Where CGCM projections typically have horizontal resolutions that vary between 100 km and 300 km, the DEWFORA projections have been designed to have horizontal resolutions in the order of 50 km, with further downscaling to 8 km resolution over selected parts of the Niger and Blue Nile river basins. Such simulations would be suitable to provide forcing to the hydrological models that are to be integrated over these two river basins as part of the project research (D3.5), and will additionally be analysed to study the changing attributes of meteorological drought over these regions (D3.6).

This document serves to describe the high-resolution projections of future climate change obtained for the African continent obtained as part of FP7 project DEWFORA. The emphasis is on describing the projected climate-change signal over the DEWFORA case study regions of the Niger and Blue Nile river basins, with the Oum-er-Rbia and Limpopo river basins (also case study regions in DEWFORA) being additional areas of interest.



2. THE REGIONAL CLIMATE MODEL AND DESIGN OF THE DOWNSCALING EXPERIMENTS

2.1 THE CONFORMAL-CUBIC ATMOSPHERIC MODEL

Regional climate modelling capacity at the CSIR Natural Resources and the Environment (NRE) is based on a variable-resolution global atmospheric model, the conformal-cubic atmospheric model (CCAM) of the Commonwealth Scientific and Industrial Research Organisation (CSIRO) in Australia. CCAM is a variable-resolution global atmospheric model, developed by the Commonwealth Scientific and Industrial Research Organisation (CSIRO) (McGregor, 1996, 2005a, 2005b; McGregor and Dix, 2001, 2008). It employs a semi-implicit semi-Lagrangian method to solve the hydrostatic primitive equations. The model employs a fairly comprehensive set of physical parameterizations. The GFDL parameterizations for long-wave and short-wave radiation are used, with interactive cloud distributions determined by the liquid and ice-water scheme of Rotstayn (1997). A stability-dependent boundary layer scheme based on Monin Obukhov similarity theory is employed (McGregor et al., 1993), together with the non-local treatment of Holtslag and Boville (1993). A canopy scheme is included, as described by Kowalczyk et al. (1994), having six layers for soil temperatures, six layers for soil moisture (solving Richard's equation) and three layers for snow. The cumulus convection scheme uses a mass-flux closure, as described by McGregor (2003), and includes downdrafts, entrainment and detrainment. CCAM may be applied at quasi-uniform resolution, or alternatively in stretched-grid mode to obtain high resolution over an area of interest.

The model code has been implemented for parallel processing using Message Passing Interface (MPI) software on the computer clusters of the CHPC. Recent years have seen the advent of variable-resolution atmospheric global circulation models such as CCAM, as an alternative to limited-area models, for the purpose of downscaling the output of CGCMs. An advantage of the variable-resolution approach is that the use of lateral boundary conditions, which are responsible for the artificial reflection of atmospheric waves in limited-area models and the occurrence of spurious vertical velocities near the boundaries, are avoided. Variable-resolution global models may therefore be considered as a specific variety of regional climate models (RCMs).

CCAM was applied in this project to simulate both present-day and future climate over Africa. The model is highly suitable for the purpose of regional climate modelling, due to its computational efficiency and variable-resolution formulation that allows great flexibility in downscaling CGCM data, through the application of a multiple nudging technique (McGregor, 2005b; Thatcher and McGregor, 2009, 2010). The model's ability to simulate the present-day characteristics of regional climate has earlier been investigated rigorously over southern Africa (e.g. Engelbrecht et al., 2009; Landman et al., 2009; Engelbrecht et al., 2012) and for various other climatological regions (e.g. Nunez and McGregor, 2007; Lal et al., 2008).

In order to obtain the ensemble of regional projections of climate change, the model was forced with the bias-corrected sea-surface temperature (SST) and sea-ice output of six different CGCMs used in AR4 of the IPCC, for the period 1961-2100. The CGCMs downscaled are:

GFDL-CM2.0 [Version 2.0 CGCM of the Geophysical Fluid Dynamics Laboratory (GFDL) of the National Oceanic and Atmospheric Administration (NOAA) in the United States];

GFDL- CM2.1 [Version 2.1 CGCM of the Geophysical Fluid Dynamics Laboratory (GFDL) of the National Oceanic and Atmospheric Administration (NOAA) in the United States];

ECHAM5/MPI-Ocean Model [The CGCM from MPI in Germany];

UKMO-HadCM3 (The Met Office Third Hadley Centre Coupled Ocean-Atmosphere GCM - United Kingdom);

MIROC3.2-medres (Model for Interdisciplinary Research on Climate 3.2, medium resolution version, of the Japanese Agency for Marine-Earth Science and Technology);

CSIRO Mark3.5 (The version 3.5 CGCM of the Commonwealth Scientific and Industrial Research Organisation in Australia).

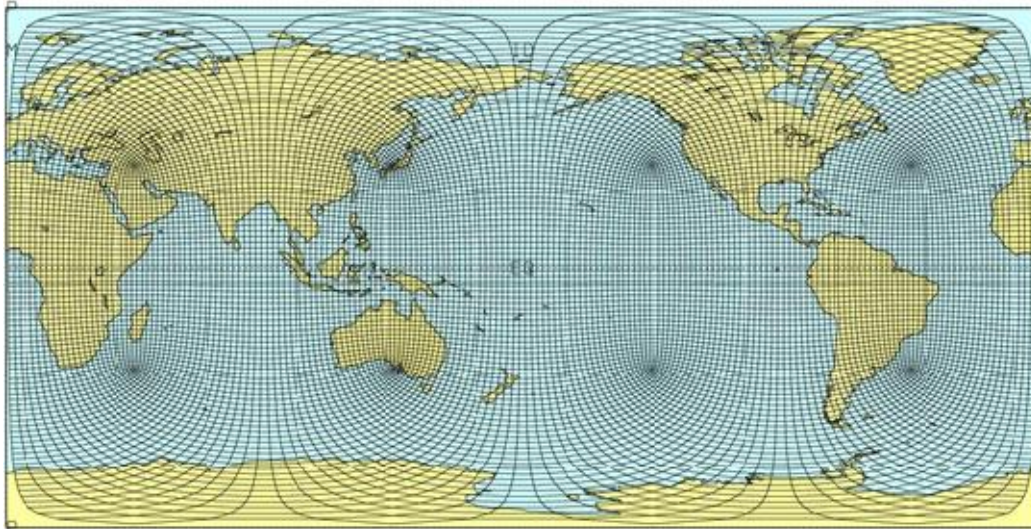


Figure 1: Quasi-uniform C48 CCAM grid, having a horizontal resolution of about 2° in latitude and longitude.

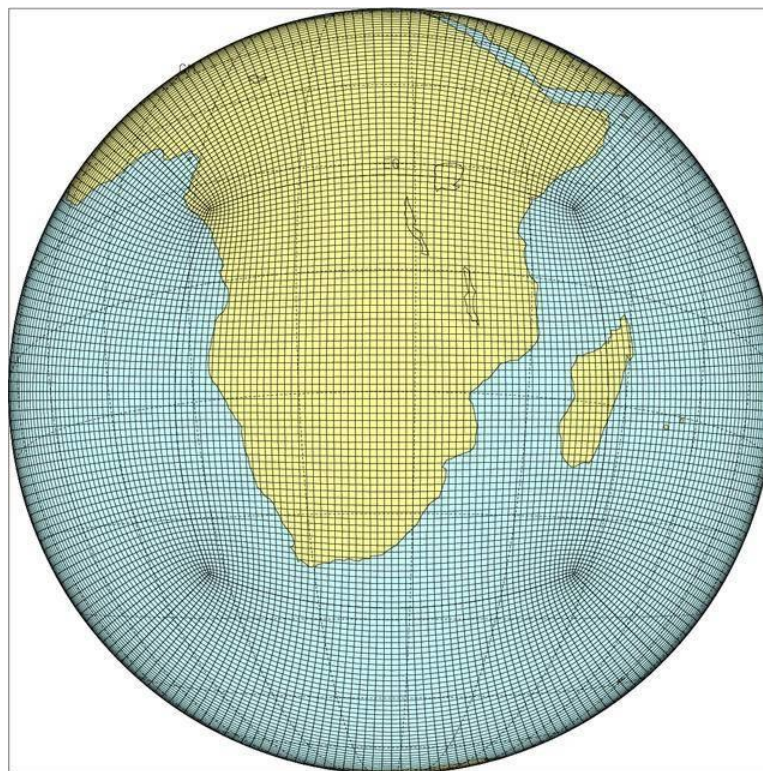


Figure 2: Stretched C64 CCAM grid, having a horizontal resolution of about 0.5° over southern Africa and the southwest Indian Ocean.

The required boundary forcing data was obtained from the CSIRO in Australia. This includes surface topography, vegetation, albedo and roughness fields required to force the model at



its lower boundary. All six of the projections performed are for the A2 emission scenario of the Special Report on Emission Scenarios (SRES). The associated CO₂, sulphate, ozone and aerosol fields were all obtained from the CSIRO. A multiple-nudging strategy was followed, by first integrating CCAM globally at quasi-uniform C48 resolution (about 200 km in the horizontal, that is, about 2° in latitude and longitude - Figure 1), forcing the model with the SSTs and sea-ice of each host model, and with CO₂, sulphate and ozone forcing consistent with the A2 scenario. In a second phase of the downscaling, CCAM was integrated in stretched-grid mode over Africa at a resolution of about 0.5° in latitude and longitude (a horizontal resolution of about 50 km – Figure 2). The higher resolution simulations were nudged within the quasi-uniform simulations, through the application of a digital filter using a 4000 km length scale. The filter was applied at six-hourly intervals and from 900 hPa upwards. An important feature of the simulations is the use of bias-corrected SSTs. A problem common to almost all CGCMs, is the existence of the “cold tongue” bias along the equatorial Pacific. This bias leads to significant distortions of atmospheric flow patterns over the equatorial Pacific in the host CGCMs (e.g. Katzfey et al., 2009; McGregor et al., 2011). The use of bias-corrected SSTs in the simulations described here avoids these distortions in the simulated atmospheric flow, and makes feasible more realistic simulations of the global and also African climate.

2.2 BIAS-CORRECTION PROCEDURE

Climate models, including both CGCMs and RCMs, are known to display systematic errors (biases) in their simulations of present-day climate attributes. For some applications (e.g. hydrological modelling) and before analysing certain aspects of the projected climate-change signal (e.g. heat wave days) it is essential to first remove systematic errors from the model simulations. For example, if a model systematically overestimates rainfall, direct application of the raw model data to hydrological modelling would lead to an unrealistic depiction of the hydrological cycle by the hydrological model.

A simple bias-correction procedure was applied in this research. First, the CRU TS3.1 data set of the Climatic Research Unit (CRU) was used to calculate the monthly climatologies for the variables of average daily rainfall, minimum temperature, maximum temperature, minimum relative humidity and maximum relative humidity, for the period 1961-1990. For each of the six downscalings performed, the simulated monthly climatologies were calculated for the same period. These were then used to calculate the monthly model biases (separately, for each downscaling). A bias-corrected version of each downscaling was subsequently obtained, by subtracting for each day in the simulation the relevant monthly bias - for each of the variables under consideration. In the case of rainfall, the overestimation/underestimation was expressed as a percentage, and daily rainfall totals were corrected with an appropriate fraction (rather than to subtract the relevant monthly bias). This bias-correction procedure results in the 1961-1990 climatology for each of the six downscalings to be exactly that of CRU TS3.1, however, the inter-annual variability and daily variability remains that of the downscaled simulation.

3. PROJECTIONS OF FUTURE CLIMATE CHANGE OVER AFRICA AND THE DEWFORA CASE STUDY RIVER BASINS

3.1 PROJECTED CHANGES IN AVERAGE TEMPERATURE

Most land areas, including the African continent, are projected to warm faster than the global average rate of temperature increase - largely due to the heat capacity of the landmasses



being significantly lower than that of the oceans (e.g. Christensen et al., 2007). The high-resolution projections presented here describe a consistent pattern of change – the tropics are projected to warm at about 1.5 times the global rate of temperature increase, whilst the subtropics are projected to warm at about twice the global rate of temperature increase (Figure 3). The median of the ensemble of CCAM projections indicates a temperature increase of about 1 °C to 2.5 °C over the Niger and Blue Nile river basins for the period 2011 to 2040 relative to 1961 to 1990, under the A2 scenario. For the period 2041-2071, warming of between 2 °C and 3 °C are projected for both basins (median of models). By 2071-2100 warming is projected to reach 3 °C to 4 °C over the Blue Nile basin, and 3 °C to 5 °C over the Niger basin. The largest warming (in the order of 5 °C) is projected for the northern parts of the Niger basin, consistent with a larger pattern of strong warming over the northern Sahara. This signal of rapid warming over the Blue Nile and Niger river basins is robust across the ensemble of projections, with the 10th and 90th percentiles of the projections generally within 1 °C of the median value.

At the continental scale, across the different time-slabs shown in Figure 3, somewhat smaller warming is projected for tropical Africa and for coastal areas in general, relative to the subtropical interior parts of the continent. The pattern of strong warming in the subtropics, extending to the most northern parts of the continent (but not to the most southern parts) is of great relevance to the both the Limpopo and Oum er-Rbia river basins. There is some seasonal variation in the temperature signal over Africa (Figure 4), although not nearly as drastic as over mid-latitudinal regions (Christensen et al., 2007). For both the Blue Nile and Niger river basins, the strongest warming is projected for the boreal summer (June to August, JJA) and boreal spring (March to May, MAM) seasons. Very strong warming is projected over North Africa, including the Oum er-Rbia river basin, during the boreal summer. Over southern Africa, including the Limpopo river basin, the largest temperature increases are projected to occur during the boreal spring.

The drastic temperature increases that are projected for large parts of the Niger and Blue Nile river basins under the A2 scenario – more than 4 °C for the period 2071-2100 relative to 1961-1990, are highly significant. This signifies regional warming at about twice the global rate of temperature increase, and forms part of a larger pattern of very strong warming over the northern Sahara and the subtropical parts of southern Africa. The rapid rise in temperature over the subtropical parts of the continent (in both hemispheres), compared to the rise in average global temperature, seems to be related to the strengthening of the subtropical high-pressure belt over the region in the future climate, particularly during between spring and summer in the Northern Hemisphere (e.g. Engelbrecht et al., 2009; Engelbrecht and Bopape, 2011b).

Keeping the rise in the global average near-surface temperature below 2 °C (compared to the global temperature at pre-industrial times) during the 21st century, through a binding international treaty on greenhouse gas emissions, has become a primary objective of the IPCC and the United Nations Framework Climate Change Convention (UNFCCC). It is thought that keeping the global temperature increase below this threshold may prevent “dangerous climate change”. However, the results presented here indicate that even if this target is reached, it would still imply strong warming over large parts of the Niger and Blue Nile river basins – in the order of 4 °C. The projected rapidly rising temperatures over these regions may be expected to have numerous impacts, for example on agriculture (e.g. Thornton et al., 2011), water resources (through increased evaporation), biodiversity and energy consumption (for example, the household energy demand for cooling in summer may be expected to increase, whilst the demand for warming in winter may be expected to decrease).

3.2 PROJECTED CHANGES IN RAINFALL

Figure 5 shows the projected change in annual rainfall totals (mm) over Africa for the periods 2011-2040, 2041-2070 and 2071-2100 relative to 1961-1990, as obtained from the ensemble of high-resolution CCAM projections. The 10th percentile (lower panel), median (middle panel) and 90th percentile (upper panel) of the ensemble of projected changes are shown. A number of studies have demonstrated the ability of CCAM to realistically simulate the attributes of the present-day rainfall climatology over southern Africa, including annual rainfall totals and the seasonal cycle in rainfall (Engelbrecht et al., 2009), inter-annual rainfall variability (Landman et al., 2009) and the frequency of occurrence of extreme rainfall events (Engelbrecht et al., 2012). The satisfactory simulation of these present-day attributes provides some confidence in the model projections of the future attributes of rainfall over the continent. Consistent with the ensemble of CGCM projections of AR4 of the IPCC, the projected rainfall signal shows great variation across the continent. It seems plausible that the subtropical parts of the continent (including southern Africa and the northern Sahara) will become drier in response to enhanced anthropogenic forcing (see also Christensen et al., 2007). Similarly, regions poleward of the subtropics are likely to dry – Mediterranean Africa, north of the Sahara (including the Oum er-Rbia river basin), as well as the winter rainfall region of southwestern South Africa. Conversely, there is evidence that East Africa and tropical Africa are plausible to become wetter. Projections of future changes in rainfall over West Africa (including the Sahel and Guinean coast) and the southern Sahara are more uncertain – there is more variation in the climate change signal across the CCAM ensemble members (see also Christensen et al., 2007). It is interesting to note that the patterns of rainfall change projected by the CCAM ensemble is largely stationary across the different time-slabs, but increases in amplitude as the greenhouse effect strengthens in time (Figure 5). The projected changes in seasonal rainfall totals across the African continent are shown in Figure 6, and are discussed in more detail on a regional basis in the following subsections.

3.2.1 The Blue Nile river basin and East Africa

The ensemble of CCAM projections (Figure 5) projects a robust pattern of rainfall increases over East Africa, east of Great Lakes area including the Blue Nile river basin, and extending into the Horn of Africa – consistent with the CGCM projections described in AR4 of the IPCC (Christensen et al., 2007). This signal is robust for annual rainfall totals across the ensemble members (Figure 5). Figure 6 reveals that the projected increases in annual rainfall totals over the Blue Nile river basin are largely driven by increases in precipitation during the boreal autumn (September to October, SON) and to a lesser extent during the boreal summer. Rainfall decreases are plausible to occur over this river basin during the boreal autumn, indicating the manifestation of a more extreme annual rainfall cycle over the region. Similar patterns of increases in annual rainfall totals over East Africa are described in the projections of Hulme et al. (2001), Ruosteenoja et al. (2003) and in the regional model projection of Engelbrecht et al. (2009). There is evidence that the East African monsoon may be expected to increase in intensity in response to the enhanced anthropogenic forcing and warming of the African continent (e.g. Engelbrecht et al., 2009). This is associated with the increased transport of moisture into East Africa (e.g. northern Mozambique, Tanzania and Kenia) with associated increases in precipitation.

3.2.2 The Niger river basin, West Africa and the Sahel

The CCAM projections indicate that it is plausible for most of the Niger river basin to become wetter under enhanced anthropogenic forcing. This pattern may be related to the tropics expanding polewards under climate change (Seidel et al., 2008). However, some of the ensemble members are indicative of a drier future, implicating that greater uncertainty is associated with the projections of climate change over the Niger basin (compared to the robust pattern of wetting over the Blue Nile basin). It is the boreal autumn that is the most plausible to become wetter over the Niger basin, according to the projections. Drying is projected for the North African west coast by most of the CCAM downscalings, a pattern that is consistent with the ensemble of AR4 CGCMs. North of the subtropics this drying occurs in response to the systematic poleward shift of storm tracks (e.g. Christensen et al., 2007). The



CCAM ensemble projects wetting over the southern Sahara, in response to the poleward-expanding tropical rainfall region. Off the Guinean coast to the south, and over the Sahel, the projected rainfall changes indicate a wetter future. However, the CGCM projections of AR4 displayed a great deal of variation over this region.

3.2.3 Southern Africa

Most of the CCAM ensemble members project drying for the southern African region (Figure 5) under climate change, in response to the subtropical high-pressure belt strengthening and expanding towards the south (e.g. Engelbrecht et al., 2009). Strong drying is projected for the Limpopo river basin by most ensemble members for all seasons, consistent with the strengthening of the subtropical highs and the northward displacement of the tracks of tropical lows and cyclones (Malherbe et al., 2012). Indeed, a robust pattern of drying over southern Africa is also projected by the CGCMs of AR4 of the IPCC (Christensen et al., 2007; also see Figure 2). Strengthening of the high-pressure belt in the austral winter is associated with the southward displacement of the westerly wind regime and the cold fronts that bring rainfall to the winter rainfall region of South Africa (the southwestern Cape and the Cape south coast). This is one of the most robust rainfall signals in the CCAM projections (Figure 5), and similarly for the CGCM projections of AR4 (Christensen et al., 2007).

3.2.4 Tropical Africa

The CCAM ensemble provides a robust message of increases in annual rainfall totals across the African tropics (Figure 5). The signal is robust for the boreal autumn (Figure 6), but less so for the remaining seasons. Warming is projected to be associated with an increase or little change in precipitation in the African tropics according to the ensemble of AR4 CGCMs (Christensen et al., 2007). Consistent with the AR4 projections, the CCAM ensemble's projected increases are projected to be rather small (less than 10 %).

3.2.5 Sahara

A robust pattern of drying is projected across the northern Sahara by the high-resolution CCAM ensemble (Figure 5), consistent with the ensemble of AR4 CGCMs (Christensen et al., 2007). This occurs in association with drying projected over the Mediterranean coast, and the strengthening and northward expansion of the subtropical high-pressure belt. The CCAM ensemble is indicative of quite substantial rainfall increases over the southern Sahara, whilst AR4 of the IPCC concluded that indications of the likely sign of the rainfall signal over this region are inconclusive.

3.2.6 The African Mediterranean coast

The African Mediterranean coast is expected to dry, in response to the large-scale poleward shift of the westerly wind regime and storm tracks, in conjunction with the strengthening and northward expansion of the subtropical high-pressure belt. This signal is robust across the ensemble of CGCM simulations described in AR4, with the rainfall decreases projected to be in the order of 20%. The CCAM ensemble consistently indicates a robust message of drastic decreases in precipitation over the Mediterranean coast and adjacent interior (including the Oum er-Rbia river basin), as large as 40% over some regions.

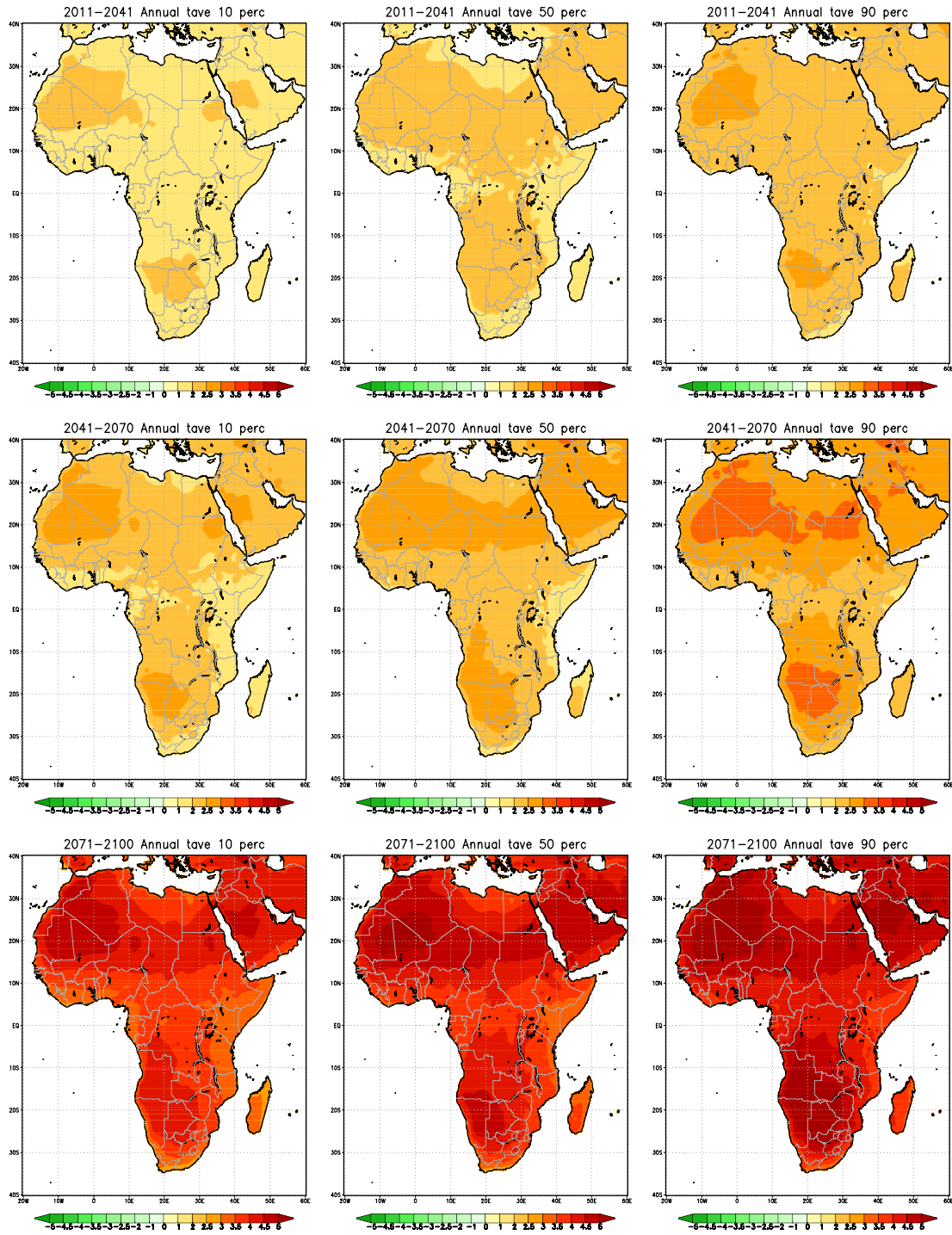




Figure 1. Projected change in the annual average maximum temperature over Africa ($^{\circ}\text{C}$), for the periods 2011-2040, 2041-2070 and 2071-2100, relative to 1961-1990. The 90th percentile (upper panel), median (middle panel) and 10th percentile (lower panel) are shown for an ensemble of six downscalings of CGCM projections, for each of the time-slabs. The downscalings were generated using the regional model CCAM. All the CGCM projections contributed to AR4 of the IPCC and are for the A2 SRES scenario.

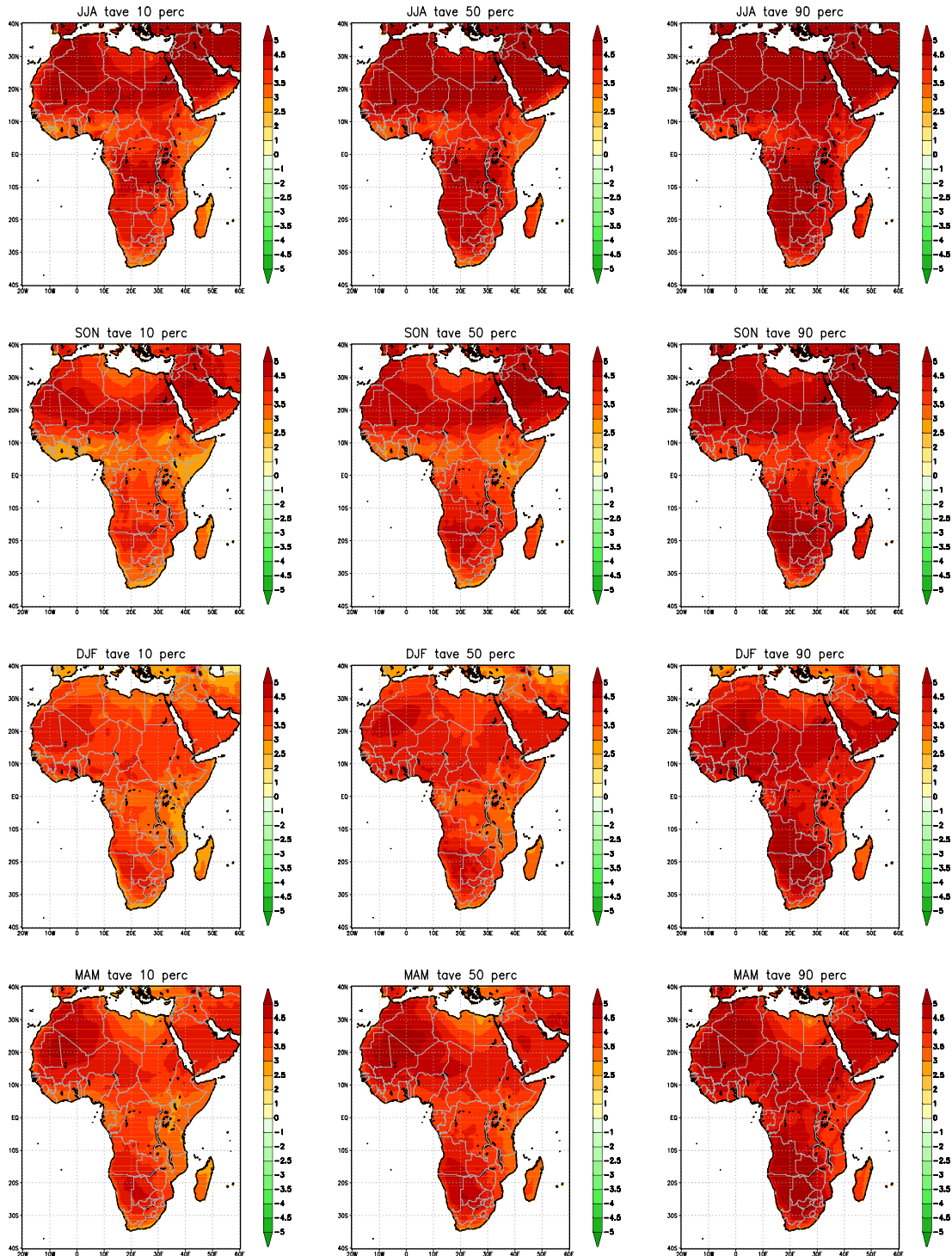


Figure 2. Projected change in the seasonal average maximum temperatures over Africa ($^{\circ}\text{C}$), for the period 2071-2100, relative to 1961-1990. The 90th percentile (upper panels), median (middle panels) and 10th percentile (lower panels) are shown for an ensemble of six downscalings of CGCM projections, for each of the seasons. The downscalings were generated using the regional model CCAM. All the CGCM projections contributed to AR4 of the IPCC and are for the A2 SRES scenario.

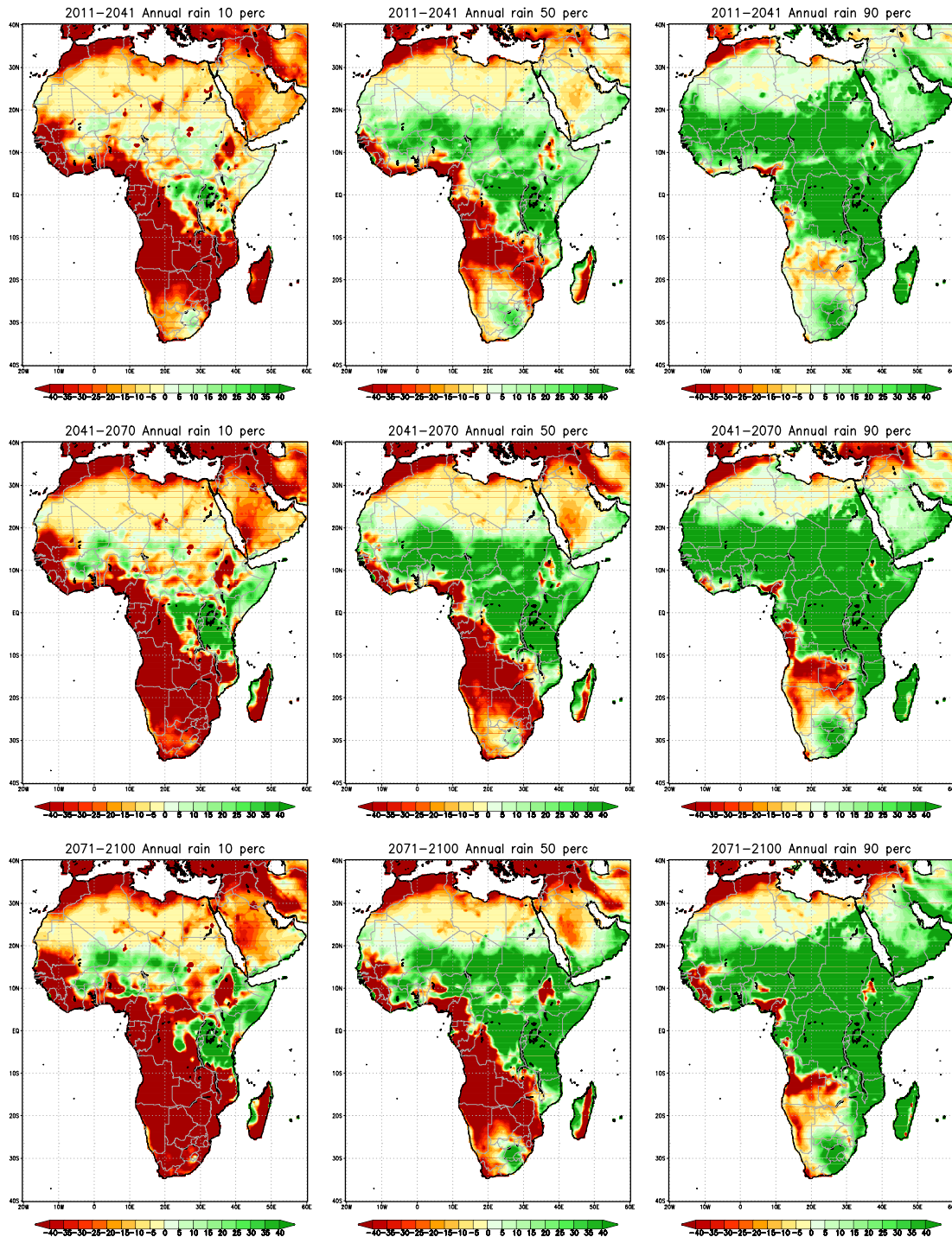


Figure 3. Projected change in the total annual rainfall (mm) over Africa, for the periods 2011–2040, 2041–2070 and 2071–2100, relative to 1961–1990. The 90th percentile (upper panel), median (middle panel) and 10th percentile (lower panel) are shown for an ensemble of six downscalings of CGCM projections, for each of the time-slabs. The downscalings were generated using the regional model CCAM. All the CGCM projections contributed to AR4 of the IPCC and are for the A2 SRES scenario.

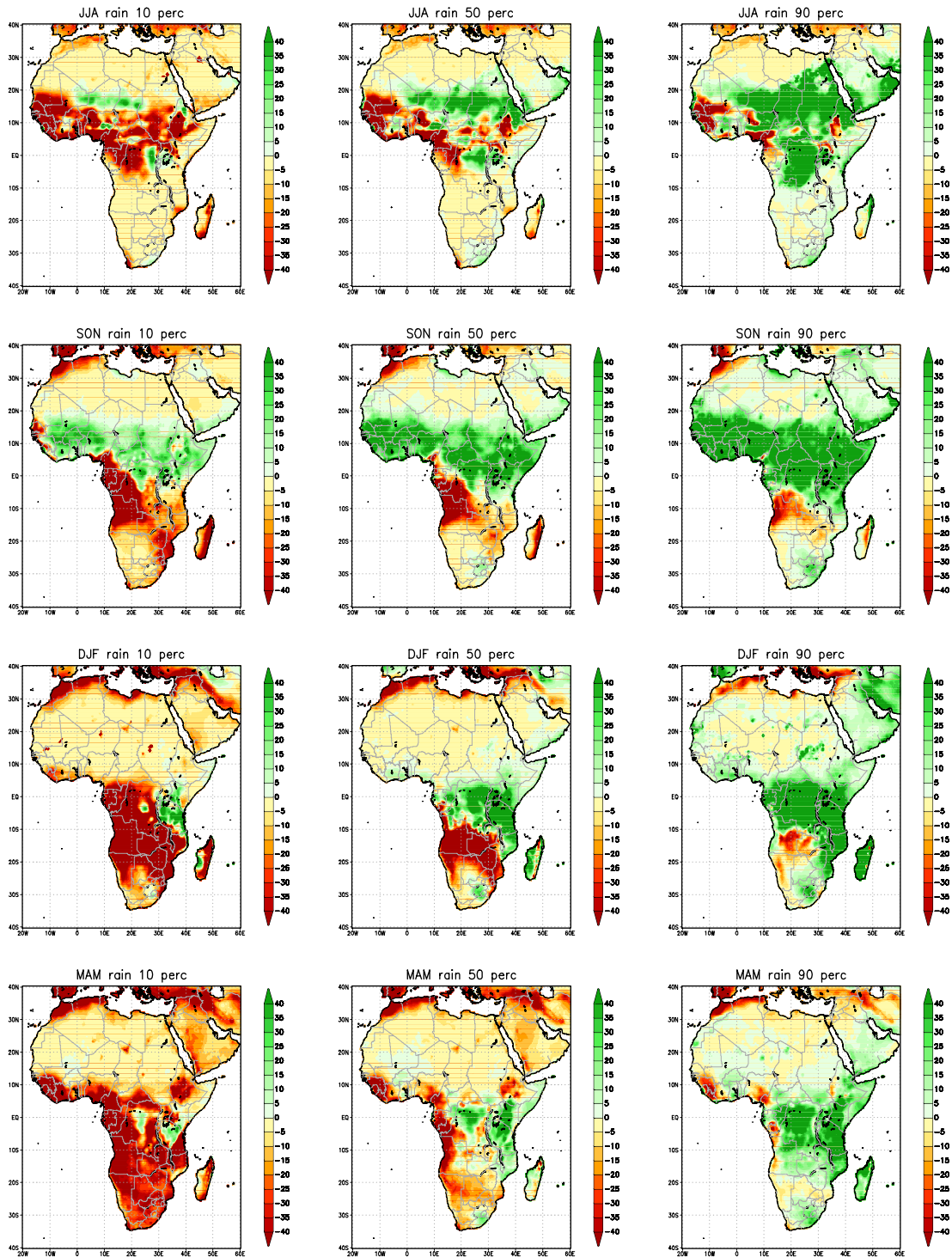


Figure 4. Projected change in seasonal rainfall totals (mm) over Africa, for the period 2071-2100 relative to 1961-1990. The 90th percentile (upper panels), median (middle panels) and 10th percentile (lower panels) are shown for an ensemble of six downscalings of CGCM projections, for each of the seasons. The downscalings were generated using the regional model CCAM. All the CGCM projections contributed to AR4 of the IPCC and are for the A2 SRES scenario.

4. PROJECTED CHANGES IN EXTREME EVENTS

The African continent exhibits a high degree of natural climate variability, and is prone to the sporadic occurrence of droughts and floods. Flooding may result from a number of different weather systems. Tropical cyclones are perhaps the most devastating; however, these systems make landfall over Africa rather infrequently, and only over the eastern coastal areas of Mozambique and South Africa (Malherbe et al., 2011). Other types of tropical systems, such as mesoscale convective complexes, typically cause flooding over tropical and subtropical Africa. Weather systems from the westerly wind regime, mostly cut-off lows, frequently bring damaging floods to the southern parts of South Africa. At the other end of the scale, dry spells, heat waves and prolonged periods of agricultural drought also occur sporadically as part of the natural climate of the continent, often in association with ENSO events. Climate change over Africa may manifest itself not only in a change in the long-term mean seasonal rainfall, temperature and circulation patterns (as described in the previous sections), but also through an increase in the frequency of occurrence of extreme events. However, the IPCC pointed out in AR4 that research on potential changes in extreme weather events over Africa is limited.

The projected change in the frequency of occurrence of extreme rainfall events (here defined as 20 mm of rain falling within 24 hours over an area of $0.5^\circ \times 0.5^\circ$) is shown in Figure 7 (10th percentile, median and 90th percentile of the ensemble of CCAM projections across various time slabs). The figure indicates a robust signal of an increase in extreme rainfall events over tropical Africa and to a lesser extent East Africa – consistent with a general (global) increase in such events that is projected to occur in association with an increase in water vapor in a warmer atmosphere. This pattern is robust across the various seasons and for both the Niger and Blue Nile river basins (Figure 8). The ensemble of CGCM projections described in AR4 of the IPCC indeed indicates that extremely wet seasons are projected to increase over both East Africa and West Africa (Christensen et al., 2007).

Extreme rainfall events are projected to decrease in frequency over parts of southern Africa (Namibia, Zambia, Botswana and Zimbabwe) and the northern Sahara – consistent with the general patterns of drying projected for these regions (Figure 3). This signal is robust for the southern African region (including the Limpopo river basin) in the ensemble of projections, but is not well-established in the 90th percentile of the ensemble over the northern Sahara (and also further to the north, over the African Mediterranean including the Oum er-Rbia river catchment). Over South Africa a projected increase in the frequency of extreme rainfall events is found consistent with earlier studies (e.g. Tadross et al., 2005; Engelbrecht et al., 2011; Engelbrecht et al., 2012) – despite the general decrease in precipitation that is projected for this region. The increase in extreme events may be at least partially be ascribed to the significant increase in surface temperatures over the region (Figure 3). Such an increase in surface temperature would be conducive to a deepening of the continental heat low, and a subsequent increase in the occurrence of heat convection and convective rainfall. In fact, a general decrease in the frequency of cut-off lows over southern Africa has been projected in previously performed simulations (see

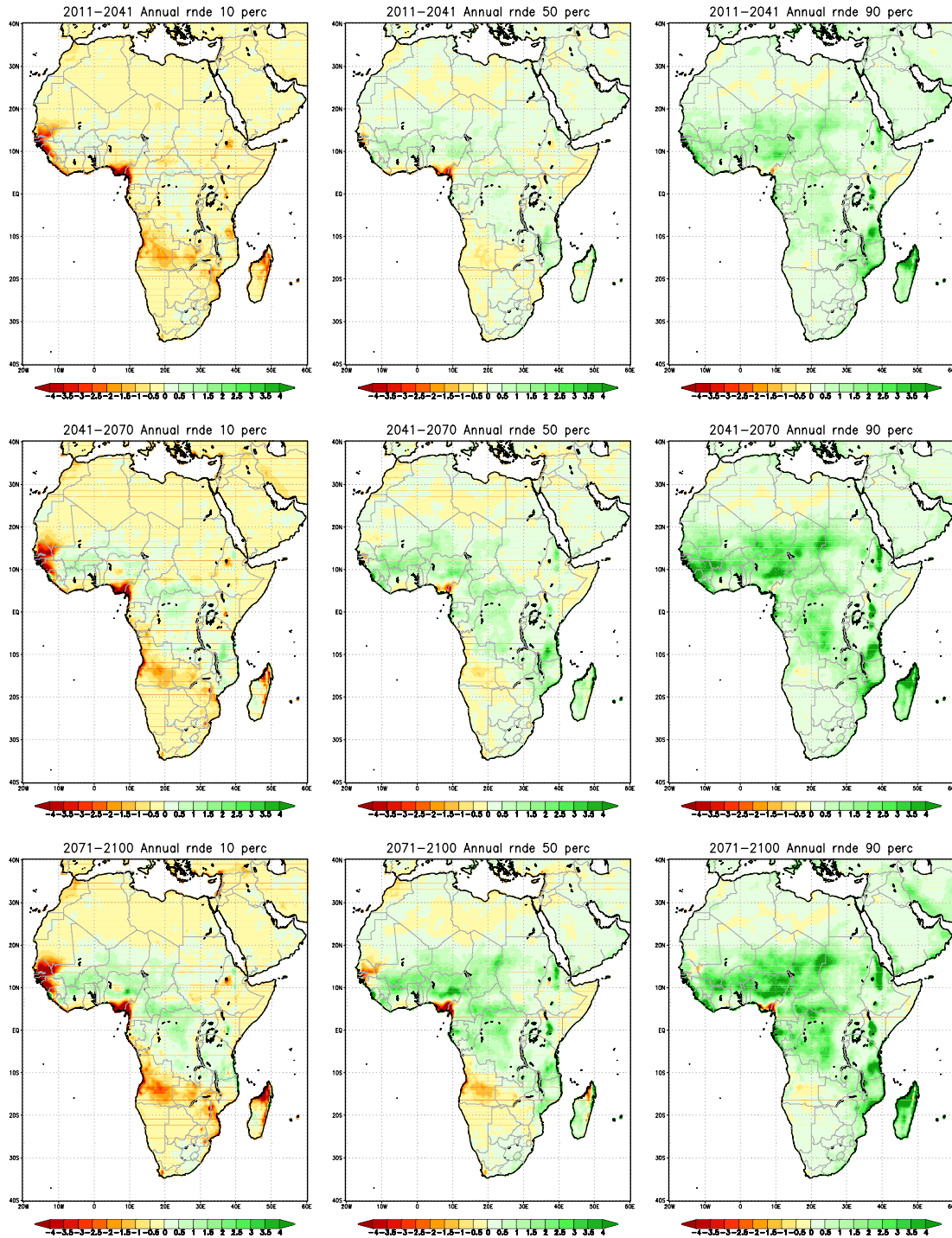


Figure 5. Projected change in the annual frequency of occurrence of extreme rainfall events over Africa, for the periods 2011-2040, 2041-2070 and 2071-2100, relative to 1961-1990. The 90th percentile (upper panel), median (middle panel) and 10th percentile (lower panel) are shown for an ensemble of six downscalings of CGCM projections, for each of the time-slabs. The downscalings were generated using the regional model CCAM. All the CGCM projections contributed to AR4 of the IPCC and are for the A2 SRES scenario. Units are the number of events per grid point per year.

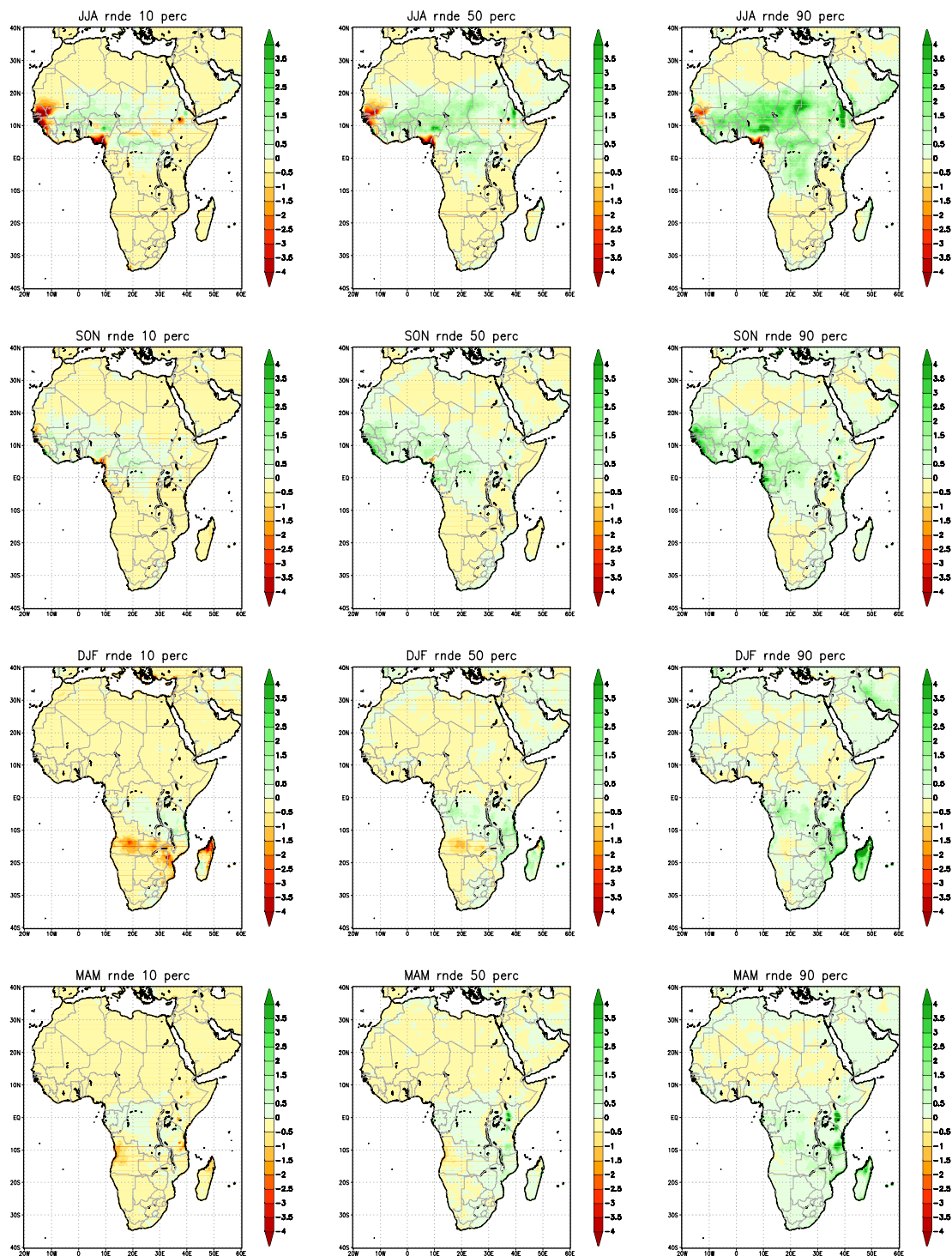


Figure 6. Projected change in the seasonal frequency of occurrence of extreme rainfall events over Africa, for the period 2071-2100 relative to 1961-1990. The 90th percentile (upper panel), median (middle panel) and 10th percentile (lower panel) are shown for an ensemble of six downscalings of CGCM projections, for each of the seasons. The downscalings were generated using the regional model CCAM. All the CGCM projections contributed to AR4 of

the IPCC and are for the A2 SRES scenario. Units are the number of events per grid point per year.

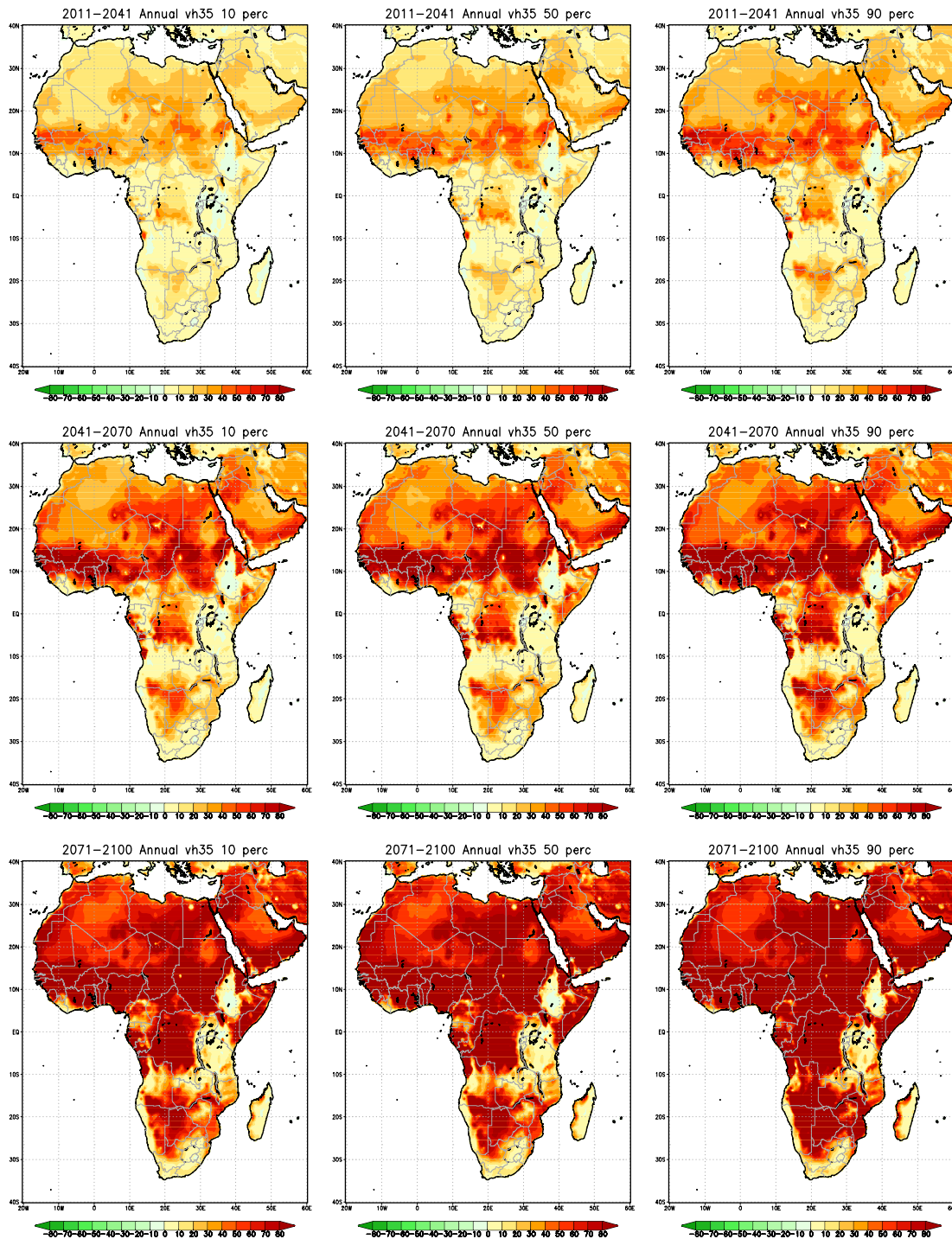


Figure 7. Projected change in the annual frequency of occurrence of very hot days over Africa, for the periods 2011-2040, 2041-2070 and 2071-2100, relative to 1961-1990. The 90th percentile (upper panel), median (middle panel) and 10th percentile (lower panel) are shown for an ensemble of six downscalings of CGCM projections, for each of the time-slabs. The

downscalings were generated using the regional model CCAM. All the CGCM projections contributed to AR4 of the IPCC and are for the A2 SRES scenario. Units are the number of events per grid point per year.

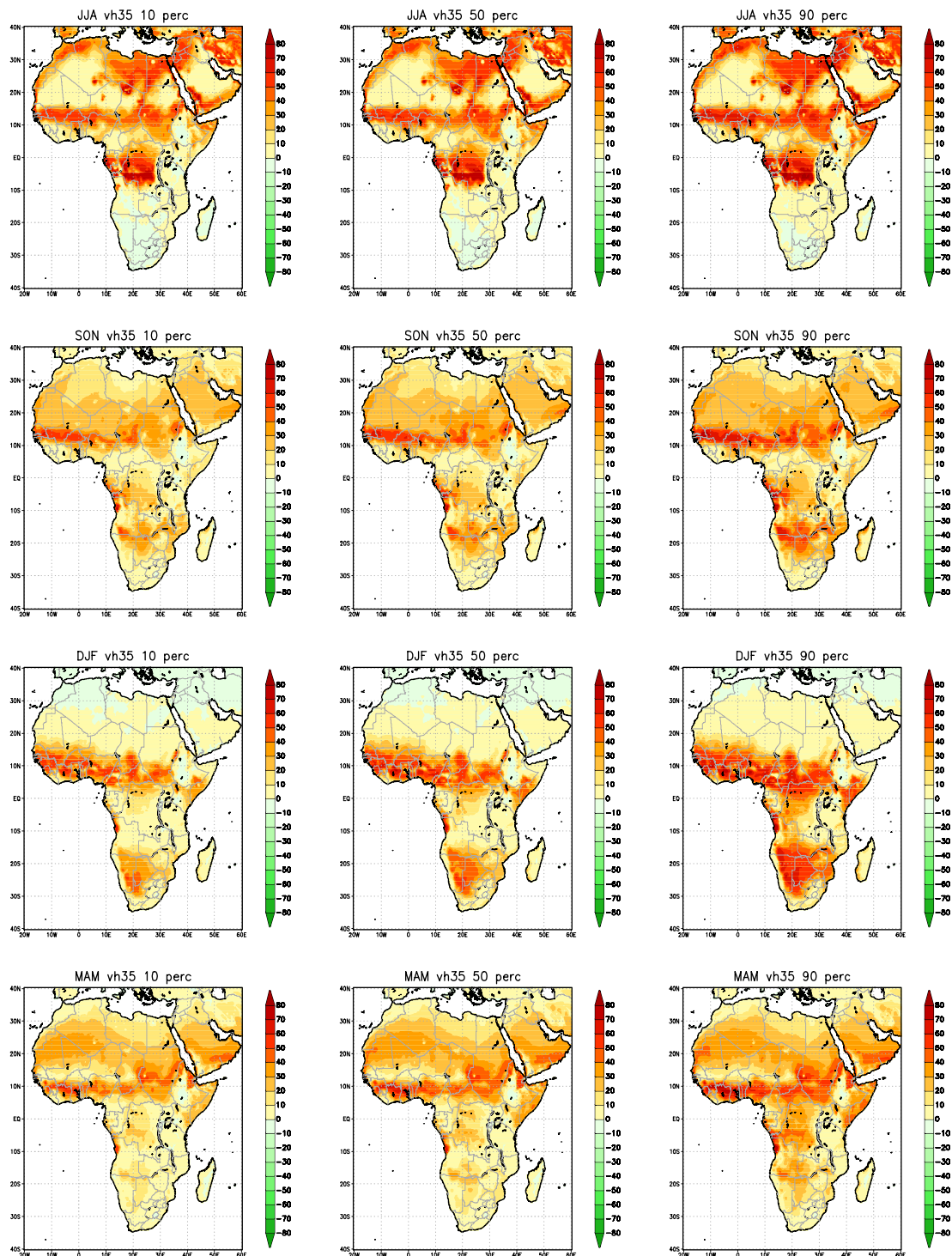


Figure 8. Projected change in the seasonal frequency of occurrence of very hot days over Africa, for the period 2071-2100, relative to 1961-1990. The 90th percentile (upper panel), median (middle panel) and 10th percentile (lower panel) are shown for an ensemble of six downscalings of CGCM projections, for each of the seasons. The downscalings were generated using the regional model CCAM. All the CGCM projections contributed to AR4 of



the IPCC and are for the A2 SRES scenario. Units are the number of events per grid point per year.

Engelbrecht et al., 2012). This suggests that the projected increase in extreme precipitation events over South Africa is the result of an increase in convective rainfall events, rather than in the widespread occurrence of heavy rainfall, as induced by cut-off lows.

The IPCC pointed out in AR4 that potential changes in the frequency of occurrence tropical cyclones over the southwestern Indian Ocean have not been investigated rigorously through modelling studies. Only a single study addressing this topic was available for inclusion in AR4. This found a significant reduction in the frequency of tropical storms in the Indian Ocean under future forcing, using a high-resolution AGCM for its simulations (Oouchi et al., 2006). The ensemble of projections performed at the CSIR has been analysed in detail by Malherbe et al. (2012) to determine whether enhanced anthropogenic forcing may be expected to lead to changes in the frequency of occurrence and tracks of landfalling tropical lows and cyclones over the southern Africa. Most of the downscaled CGCM projections exhibit a pattern of higher rainfall totals and an increase in extreme rainfall events over the Indian Ocean to the north of Madagascar and over northern Mozambique (Figures 2 and 3). This is indicative of a northward shift in the preferred location of tropical low and cyclone tracks, as induced by a strengthening of the Indian Ocean High over the southwest Indian Ocean during the late summer – see Malherbe et al. (2012) for a detailed discussion of the underlying circulation dynamics. The general drying that is projected over north-eastern South Africa and the Limpopo river basin during the summer and autumn (Figure 3), is partially the result of the northward displacement of tropical low and cyclone tracks over the southwestern Indian Ocean (Malherbe et al., 2012).

Drastic increases in the annual and seasonal frequency of occurrence of very hot days (here defined as days when the maximum temperature exceeds 35° C) are projected (Figures 9 and 10) across the African continent. This figure shows the 10th percentile, median and 90th percentile of the projected change in very hot days across the ensemble. The projected pattern of change is robust. The largest increases in very hot days (increases of more than 100 very hot days per year for 2071-2100 relative to 1961-1990) are projected to occur over southern Africa (including the Limpopo river basin), the western tropics and southern Sahara (including the Niger river basin) and the eastern part of North Africa (Figure 9). The relatively small increases over the northern Sahara may be attributed to the relatively high occurrence of such days in the present-day climate. Relatively small increases in the number of very hot days are also projected over the eastern escarpment areas of South Africa and the highlands of East Africa.

5. CONCLUSIONS

Six different CGCM projections of future climate change over Africa have been downscaled to high resolution (50 km in the horizontal) over the African continent, for the period 1961-2100. All six CGCM projections were for the A2 scenario contributed to AR4 of the IPCC. These simulations were subsequently bias-corrected, using the monthly climatologies of rainfall, average temperature and relative humidity of the CRU TS3.1 data set. The projections indicate that drastic climate change, particularly temperature increases, are plausible to occur over Africa during the 21st century, should emissions increase according to or faster, as described in the A2 scenario. The median temperature increase for 2071 to 2100, compared to 1961-1990, varies between 3 and 5 °C across the continent in the CCAM projections. The subtropical regions of the continent (southern Africa and the northern Sahara) are projected to warm most, at a rate of about twice the global rate of temperature increase. That is, drastic increases in surface temperature are likely over the subtropical parts of the continent, even if the UNFCCC would be successful in restraining the global increase in temperature to 2° C.



Although the projections of future rainfall changes over the continent show considerable variation across the continent, there are robust signals of some large-scale changes in the CCAM projections. The subtropical parts of the continent (southern Africa and the northern Sahara) are projected to become drier, with even more drastic decreases in rainfall projected for the extra-tropical margins of the continent – the Mediterranean coast of North Africa, and the southwestern Cape and Cape south coast of South Africa. These changes seem to be driven by the strengthening of the subtropical highs in each of the hemispheres, with an associated poleward displacement of the westerly wind regime. There is also a robust signal of East Africa becoming wetter in response to the strengthening of the East African monsoon. More uncertainty surrounds the CCAM projections of future climate change over West Africa and the Sahel, where many CGCMs fail to simulate realistically key aspects of African climate – such as the West African monsoon (e.g. Christensen et al., 2007).

The CCAM projections provide evidence that the frequency of occurrence of very hot days is likely to increase across the continent, and in particular over subtropical southern Africa, the western tropics and North Africa. This is to occur in association with the strengthening of the subtropical highs and the poleward displacement of the westerly wind regime, with associated decreases in rainfall over large parts of the continent. It is likely that extreme rainfall events will increase in frequency across the tropics, in response to the general increase in moisture in the warmer atmosphere. Over East Africa, where the monsoon is projected to strengthen, robust increases in precipitation are projected. Similarly, rainfall increases are projected over the northern parts of Mozambique, due to a northward displacement of tropical cyclone tracks.

The Niger river basin is projected to experience rapid temperature rise during the 21st century, under the A2 scenario. The median of the CCAM ensemble projects temperature increases ranging ranging from 3 °C in the south to 5 °C in the north, under the A2 scenario – a robust message of change across the ensemble members. An associated increase in very hot days (80 days per year or more) is projected for the basin. Such drastic increases in both the average temperature and extreme temperature days are likely to impact negatively on crop yield and the hydrological cycle in the basin (through enhanced evaporation). It is plausible, however, for the basin to experience increases in both annual average rainfall and extreme rainfall events, under enhanced anthropogenic forcing.

The CCAM ensemble projects a robust message of annual rainfall increases, and increases in extreme precipitation events, over the Blue Nile river basin. These increases are projected to occur in response to a strengthening of the East African monsoon. Compared to the Niger basin, less drastic increases in temperature and very hot days are projected for the Blue Nile basin, to some extent as a result of the simulated increases in cloud cover and rainfall over this region.

6. REFERENCES

Christensen et al. 2007. Regional Climate Projections. In: *Climate Change 2007: The Physical Science Basis. Contribution of Working Group I to the Fourth Assessment Report of the Intergovernmental Panel on Climate Change*. Cambridge University Press, Cambridge, United Kingdom and New York, NY, USA.

Engelbrecht CJ. Engelbrecht FA. Dyson LL. 2012. High-resolution model-projected changes in mid-tropospheric closed-lows and extreme rainfall events over southern Africa. *International Journal of Climatology*. DOI: 10/1002/joc.3420.

Engelbrecht FA. McGregor JL. Engelbrecht CJ. 2009. Dynamics of the conformal-cubic atmospheric model projected climate-change signal over southern Africa. *International Journal of Climatology* **29**, 1013-1033.



Engelbrecht FA. Bopape MM. 2011. High-resolution projected climate futures for southern Africa. SASAS conference, Pretoria, South Africa, 21-22 September 2011.

Hewitson BC. Crane RG. 2006. Consensus between GCM climate change projections with empirical downscaling: precipitation downscaling over South Africa. *Int. J. Climatol.* **26**, 1315-1337.

Hulme M. Doherty R. Ngara T. 2001. African climate change: 1900-2100. *Clim. Res.* **17**, 145-168.

Katzfey JJ. McGregor JL. Nguyen KC. Thatcher M. 2009. Dynamical downscaling techniques: Impacts on regional climate change signals. In: Anderssen RS, Braddock RD and Newham LTH (eds.). MODSIM09 Int. Congress on Modelling and Simulation. URL: www.mssanz.org.au/modsim09/113/katzfey_113.pdf 2377-2383.

Kowalczyk E A, Wang, Law RM, Davies HL, McGregor JL and Abramowitz G (2006) The CSIRO Atmosphere Biosphere Land Exchange (CABLE) model for use in climate models and as an offline model. CSIRO Marine and Atmospheric Research Paper 13, 37 pp.

Lal M. McGregor JL. Nguyen KC. 2008. Very high resolution climate simulation over Fiji using a global variable-resolution model. *Climate Dynamics* **30**, 293-305.

Landman WA. Engelbrecht FA. Beraki A. Engelbrecht C. Mbedzi M. Gill T. Ntsangwane L. 2009. Model output statistics applied to multi-model ensemble long-range forecasts over South Africa. Water Research Commission Report, No 1492/1/08. 56 pp.

Malherbe J. Engelbrecht FA. Landman WA. Engelbrecht CJ. 2011. Tropical systems from the southwest Indian Ocean making landfall over the Limpop River Basin, southern Africa: a historical perspective. *International Journal of Climatology*. DOI: 10.1002/joc.2320.

Malherbe J. Engelbrecht FA. Landman WA. 2012. Projected changes in tropical cyclone climatology and landfall in the southwest Indian Ocean region under enhanced anthropogenic forcing. *Climate Dynamics*. DOI: 10.1007/s00382-012-1635-2.

McGregor JL (1996) Semi-Lagrangian advection on conformal-cubic grids. *Mon. Wea. Rev.* **124** 1311-1322.

McGregor JL (2003) A new convection scheme using a simple closure. In "Current issues in the parameterization of convection", BMRC Research Report 93, 33-36.

McGregor JL (2005a) Geostrophic adjustment for reversibly staggered grids. *Mon. Wea. Rev.*, **133**, 1119-1128.

McGregor JL (2005b) C-CAM: Geometric aspects and dynamical formulation. CSIRO Atmospheric research Tech. Paper No. 70, 43 pp.

McGregor JL and Dix MR (2001) The CSIRO conformal-cubic atmospheric GCM. In IUTAM Symposium on Advances in Mathematical Modelling of Atmosphere and Ocean Dynamics, P. F. Hodnett (Ed.), Kluwer, Dordrecht, 197-202.

McGregor JL and Dix MR (2008) An updated description of the Conformal-Cubic Atmospheric Model. In *High Resolution Simulation of the Atmosphere and Ocean*, eds. K. Hamilton and W. Ohfuchi, Springer, 51-76.

McGregor JL. Katzfey JJ. Nguyen KC. Thatcher MJ. 2011. Some recent developments for dynamic downscaling of climate. Proc. 27th Annual Conference of the South African Society for Atmospheric Sciences. September 2011, Hartebeesboek.

Meadows ME. 2006. Global change and southern Africa. *Geographical Research* **44**, 135-145.

Nunez M. and McGregor J.L. (2007). Modelling future water environments of Tasmania, Australia. *Climate Research* **34** 25-37.



Olwoch JM. Reyers B. Engelbrecht FA. Erasmus BFN. 2008. Climate change and the tick-borne disease, Theileriosis (East Coast fever) in sub-Saharan Africa. *Journal of Arid Environments* **72**, 108-120.

Oouchi K et al. 2006. Tropical cyclone climatology in a global-warming climate as simulated in a 20 km-mesh global atmospheric model: Frequency and wind intensity analysis. *J. Meteorol. Soc. Japan* **84**, 259-276.

Rotstayn LD (1997) A physically based scheme for the treatment of stratiform clouds and precipitation in large-scale models. I: Description and evaluation of the microphysical processes. *Quart. J. Roy. Meteor. Soc.*, 123 1227-1282.

Ruosteenoja K. Carter TR. Jylha K. Tuomenvirta H. 2003. Future Climate in World Regions: An Intercomparison of Model-Based Projections for the New IPCC Emissions Scenarios. Finnish Environment Institute, Helsinki, 83 pp.

Seidel DJ. Fu Q. Randel WJ. Reichler TJ. 2008. Widening of the tropical belt in a changing climate. *Nature Geoscience* **1**, 21-24.

Tadross M. Jack C. Hewitson B. 2005. On RCM-based projections of change in southern African summer climate. *Geophysical Research Letters* **32**, L23713. DOI: 10.1029/2005GL024460.

Thatcher M. McGregor JL. 2009. Using a scale-selective filter for dynamical downscaling with the conformal cubic atmospheric model. *Monthly Weather Review* **137**, 1742-1752.

Thatcher M. McGregor JL. 2010. A technique for dynamically downscaling daily-averaged GCM datasets over Australia using the Conformal Cubic Atmospheric Model. *Monthly Weather Review* **139**, 79-95.

Thornton PK. Jones PG. Ericksen PJ. Challinor AJ. 2011. Agriculture and food systems in sub-Saharan Africa in a 4 C+ world. *Phil. Trans. R. Soc.* **369**, 117-136. DOI: 10.1098/rsta.2010.0246.